Effect of Beams Structures on Dynamic Behavior of Piezoresistive Accelerometer Sensors

Norliana Yusof[1], Norhayati Soinb[2] and Abdullah C.W Noorakma[1]
[1]*Faculty of Innovative Design and Technology,*
Universiti Sultan Zainal Abidin, Gong Badak Campus, 21300 Kuala Terengganu.
[2]*Department of Electrical Engineering,*
Faculty of Engineering, University of Malaya, 50603 Kuala Lumpur.
norliana@unisza.edu.my

***Abstract*—This paper presents the design and simulation analysis of MEMS piezoresistive accelerometer sensor which can be used as airbag sensors. In this study, five different shapes of accelerometer structures with identical proof mass volume are designed and simulated by using Comsol Multiphysics software. The static analysis and modal analysis were conducted to investigate the stress, displacement, strain and resonant frequency of each structure. From the static analysis, it can be observed that structure with four beams parallel to the proof mass and attached at the edge of it, perform the highest value of stress, 6.78 X10^8 N/m^2. In this study, the minimum natural frequency of 2 kHz is chosen as a hard constraint in order to obtain a bandwidth at least of 400 Hz to meet requirements for airbag application. From the modal analysis, the structure with four beams connected in the middle of each of the four sides of the proof mass and the structure with eight beams surrounding the proof mass has demonstrated more than the acceptable natural frequency with 6.79 kHz and 2.00 kHz respectively. From this study, it has been shown that the structure with a proof mass surrounded by eight beams is the best choice for achieving maximum mechanical sensitivity and desirable resonant frequency for airbag sensor applications.**

***Index Terms*—Static Analysis; Dynamic Analysis; MEMS Piezoresistive Accelerometer Sensor; COMSOL Multiphysics.**

I. INTRODUCTION

Over past 30 years, a MEMS accelerometer has been used in various field including automotive, industrial and medical. In automotive applications, they are widely used in safety systems, such as airbags, improvement vehicle stability systems and electronic suspension, to name a few [1]. Piezoresistive, capacitive and piezoelectric are commonly used as sensing principles to convert acceleration into the electrical signal; with each sensing principle having its advantages and limitations. MEMS Piezoresistive accelerometers are commonly used due to its simple structure, simple fabrication process and read out circuit compared to other accelerometers [2].

Most of the studies carried out by few researchers have proposed their distinctive shape of MEMS Piezoresistive sensors and used different types of material and fabrication process. This has led to the investigation of best shape (simple structure with high sensitivity) of a wide range of structurally diverse shape proposed amongst MEMS Piezoresistive accelerometers design for airbag deployment system. A Piezoresistive Accelerometer consists of the central proof mass suspended by supported beams that are fixed to an outer frame or anchor. Acceleration will cause a force to act on the proof mass, which is consequently deflected by a distance, x as illustrated in Figure 1.

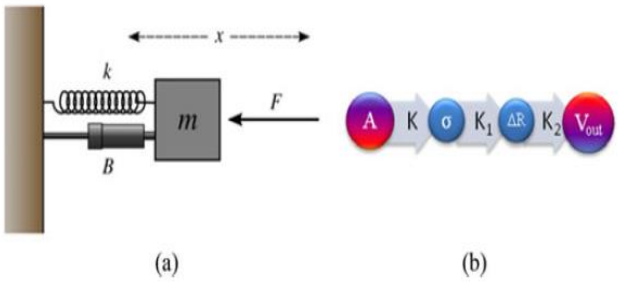

Figure 1: Piezoresistive Accelerometer Sensing Principle [3]

Piezoresistive Accelerometer measures the electrical resistance of material when mechanical stress, which is proportional to inertial force is applied. Piezoresistors are diffused inside the beams structure and strain effect on the flexures or beams determines a change in resistance of piezoresistors (gauges) which is connected electrically in a Wheatstone bridge circuit. The performance of microaccelerometers can be achieved when the resonant frequency and the sensitivity requirements are fulfilled [4]. The accelerometer performance can be characterized as static performance which is the sensitivity and dynamic performance that includes bandwidth, damping, etc. [5]. A major optimization on the sensitivity can be achieved by selecting an appropriate structure of the accelerometer. There are many factors that will affect the performance of MEMS accelerometer sensors, including shape and geometry of proof mass and beams, piezoresistors, power consumption, temperature coefficient and the Wheatstone bridge [6][7]. The beam is one of an important part of an accelerometer as it will determine the stiffness constant, k [8]. One of the effective ways to reduce the cross-axis sensitivity is by increasing the number of support beams. But if there are too many beams, the primary axis sensitivity will decrease significantly since they are tightly constraining the movement of the central proof mass [9]. The sensitivity can also be improved if the proof mass is made larger or the piezoresistors and beams made as thin as possible [5]. To improve the sensitivity, the various shapes of MEMS Piezoresistive sensors have been proposed that include symmetrical [2][6][9][10][11][12][13][14] and non-symmetrical structures [15][16]. The disadvantage of a non-symmetry structure is the large transverse sensitivity caused by the asymmetric mass distribution whereby the symmetric

design may solve the problem [12]. Hence, this study focuses on symmetrical design structures due to this advantage. A simple quad-beam structure consists of a proof mass suspended by four thin flexures shifted toward the proof mass edges was proposed by A.Ravi et al. [2]. From their study, the shifted beams towards the proof mass edge structure require corner compensation only at the bottom compared to non-shifted beams which require at both top and bottom side of the proof mass. Corner compensation method is the most widely used technique for the fabrication of sharp convex corners [18]. From the study proposed by Yi Luo [9], the shape structure was similar to A.Ravi et al. [2], with additional of the extra four beams. Two of them are located in X-axis to enhance X-axis stiffness and the other two beams in Y-axis to gain Y-axis robustness [9]. The structure designed in the paper studied by Du Chunhui et al. [11] consists of eight beams with two beams at each center of the proof mass. Messina et al. [14] proposed the structure with proof mass suspended by four beams connected in the middle of each of the four sides of the proof mass surrounding it. While Abdel Kader et al. [10] studied the structure of the proof mass surrounded by four beams and attached at the edge of the proof mass. The objective of this paper is to investigate the effect of beam structures on dynamic parameters of MEMS Piezoresistive accelerometer including von mises stress, total displacement, strain, natural frequency and mechanical sensitivity. In this paper, five different shapes and beams structures of MEMS Piezoresistive accelerometer are investigated and the comparison of these dynamic parameters is analyzed and reported.

II. METHODOLOGY

The selected five shapes of MEMS Piezoresistive Accelerometer were designed and simulated using Finite Element Analysis (FEA) software COMSOL Multiphysics. In this study, the selected symmetrical structures were based on research done by A.Ravi et.al [2], Yi Luo [9], Du Chunhui et al. [11], Messina et al. [14] and Abdel Kader et al. [10]. Both static analysis and modal analysis were conducted by applying force on the proof mass. The target technical specifications of the accelerometer were referred to fulfill the application requirements of airbag applications. The target sensor specifications are listed in Table 1. The parameters setting for finite element analysis are set as shown in Table 2.

The various shapes addressed in this study consist of single proof mass with various beams design as shown in Figure 2. In the present designs, all the structures under study have identical proof mass volume, therefore since they are all under the same loading condition; the inertial forces applied to the beams of each structure are comparable.

Table 1
Typical Specifications of accelerometers for airbag detection system application [1]

Parameter	Value
Proof mass volume, V	1.56 x 10^{-8} m^3
Proof mass area, A	3500 µm x 3500 µm
Beam thickness, *t*	30 µm
Mass of the proof mass, m	3.625 x 10^{-5} kg
Silicon density , ρ	2330 kg / m^3
Young Modulus of silicon, E	185 GPa
Poisson's ratio of silicon, ν	0.28

Table 2
The parameters setting for finite element analysis

Parameter	Value
Range (g)	±50 g
Frequency Range	DC-400 Hz
Resolution	<100mg
Off axis Sensitivity	<5%
Non-linearity	<2%
Max Shock in 1ms	>2000g
Temperature Range	-40ºC to 85ºC
TC of offset	<60mg/ºC
TC of Sensitivity	<900ppm/ ºC

A. Static Simulation Analysis

Static analysis is conducted to verify the values of maximum stress, total displacement and strain on the beams when force is applied to the proof mass in X, Y and Z axis direction. The total force, F applied to the proof mass can be calculated by [17]:

$$F = ma \tag{1}$$

where m = mass of the proof mass and a is acceleration which is 0-50 g for airbag application. After an inertial force is applied to the proof mass, the strain on the piezoresistors changes its electrical resistance proportionally. The relation that relates the change in resistance to the relative change in stress can be expressed as [5]:

$$\frac{\Delta R}{R} = G\frac{\Delta L}{L} \tag{2}$$

where $\frac{\Delta R}{R}$ = change in resistance, G is gauge factor and $\frac{\Delta L}{L}$ is a strain of beams.

B. Modal Analysis Simulation Study

The modal analysis has been performed for five different structures to find out the value of natural frequencies. In the case of free vibration without damping, the proof mass will oscillate with simple harmonic motion with a frequency of fn (undamped natural frequency). For the simple mass spring system, fn is defined as [18]:

$$fn = \frac{1}{2\pi}\sqrt{\frac{k}{m}} \tag{3}$$

where f_n is the natural frequency, m is the mass of proof mass and k is the spring constant which defines the stiffness of the beams. The higher the natural frequency (frequency at which the device resonates), the larger the usable bandwidth of the device. In this design, the mass is constant at 3.625 x 10^{-5} kg, hence the natural frequency solely depends on the spring constant, k. It is quite difficult to determine the value of spring constant of each shapes since it depends on the Young modulus of the materials, number of beams, length, width and the distance between the beams and the center of proof mass [9] .The mechanical sensitivity, S of the structure is related to the angular frequency as [19]:

$$S = \frac{1}{w_n^2} \tag{4}$$

where the angular natural frequency, $W_n = 2\pi fn$.

This equation clarifies the trade-off to be achieved between sensitivity and natural frequency in designing the accelerometer mechanical structure for airbag application.

Shape 1
A.Ravi et al.
[2]
The proof mass is suspended by four symmetrical beams. The four beams are aligned in line with the proof mass edges.

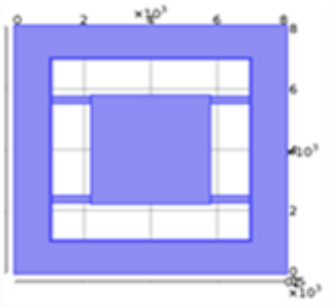

Shape 2
Yi Luo [9]

The structure is same as shape 1 with additional of the extra four beams. Two of them are located in X-axis and the other two beams in Y-axis.

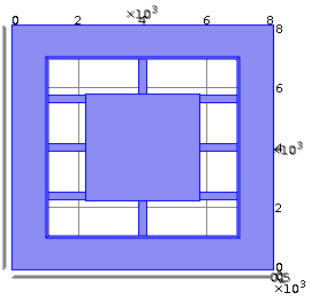

Shape 3
Du Chunhui et al.[11]

The proof mass is suspended by eight beams with two beams are attached at each center of the proof mass.

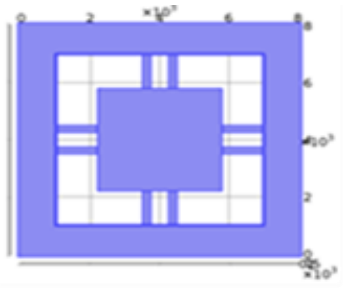

Shape 4
Messina et al. [14]

The proof mass is suspended by four beams connected in the middle of each of the four sides of the proof mass surrounding it.

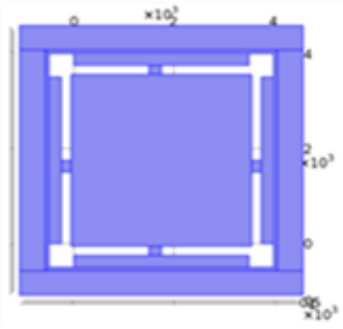

Shape 5
Abdel Kader et.al [10]

Four beams are parallel to the proof mass and attached at the edge of the proof mass.

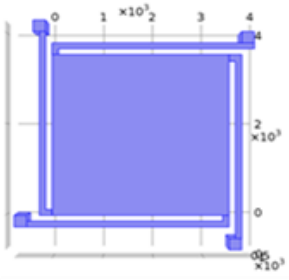

Figure 2: Various shapes addressed in this study; Shape 1 to 5

III. Simulation Results and Discussion

This section presents the simulation results and performance comparison of Shape 1 to 5 based on maximum stress, total displacement, strain, natural frequency and mechanical sensitivity.

A. Static Simulation Results

Stress profile of the accelerometer structure was analyzed to locate the maximum stress region along the beams length. Figure 3 illustrates the stress plot of five shapes of accelerometer structure under z-axis acceleration.

Shape 1

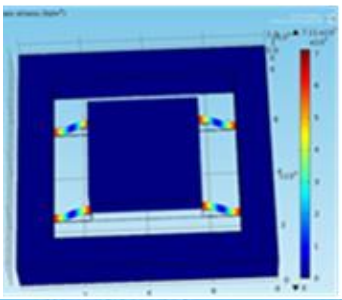

Shape 2

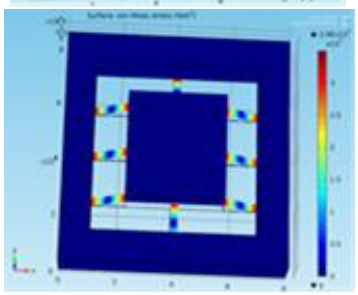

Shape 3

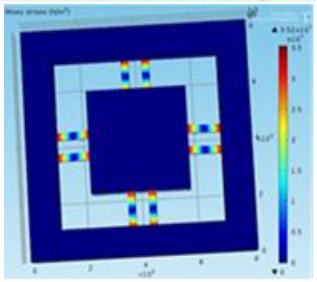

Shape 4

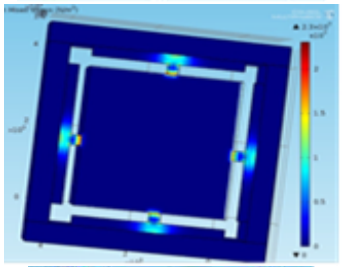

Shape 5

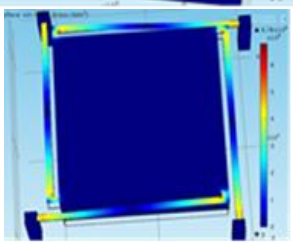

Figure 3: Stress plot of five shapes of accelerometer structure under z-axis

The red color indicator shows the maximum stress regions, while, the blue color shows the minimum stress regions. From the figure, it can be observed that the maximum stress region is located near the fixed ends of the beams and the minimum stress in the middle of the beams for shapes 1, 2 and 3. For shapes 4 and 5, the maximum stress regions are located near the mass end of the proof mass. Thus, the piezoresistors are proposed to be placed at these maximum stress regions to

maximize the piezoresistive effect [2][5][20]. Table 3 shows the performance comparison of stress, displacement, strain, natural frequency and mechanical sensitivity of five shapes structure when full scale of 50 g acceleration, under z axis was applied to the proof mass. The comparison of maximum stress for all five shapes for 0-50 g acceleration can be clearly seen from Figure 4.

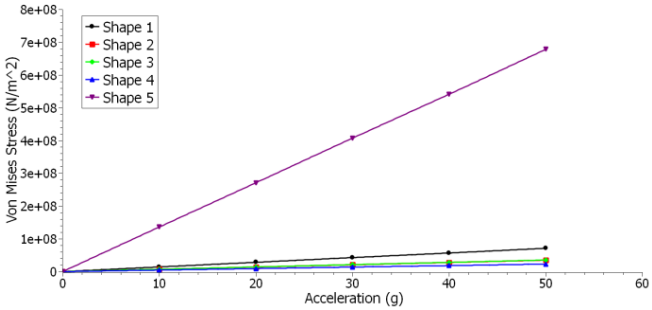

Figure 4: The comparison of maximum stress for all five shapes for 0-50 g acceleration

From the figure, the structure with four beams parallel to the proof mass and attached at the edge of it (shape number 5), performs the highest value of stress, 6.78 x10^8 N/m^2, followed in order by structure with the four beams aligned in line with the proof mass edges (shape number 1) with a stress value of 7.11x 10^7 N/m^2.

The structure with eight beams surrounding the proof mass (shape number 2 and 3) gives approximately 3.50 x 10^7 N/m^2 value of stress while the structure with four beams connected in the middle of each of the four sides of the proof mass (shape number 4), performs the lowest value of stress, 2.30 x 10^7 N/m^2 . Shape 5 also shows the significant value of maximum stress compared to the other 4 designed structures.

Figure 5 shows the comparison of strain for all five shapes at 0 - 50 g, z -axis acceleration. The figure displays the identical results for strain and maximum stress for all five shapes in which the highest strain are constrained at the beam of shape 5 followed in order shape number 1, 2 and 3, continued by shape number 4 respectively. This relation relates to the piezoresistive accelerometer sensing principle; an applied mechanical stress is proportional to the strain of the length of the beams. The value of the strain is required as it is assumed to be acting as piezoresistors' strain which is placed on the beams. Once the value of the strain is known, the change in resistance can be calculated by using the Equation (2).

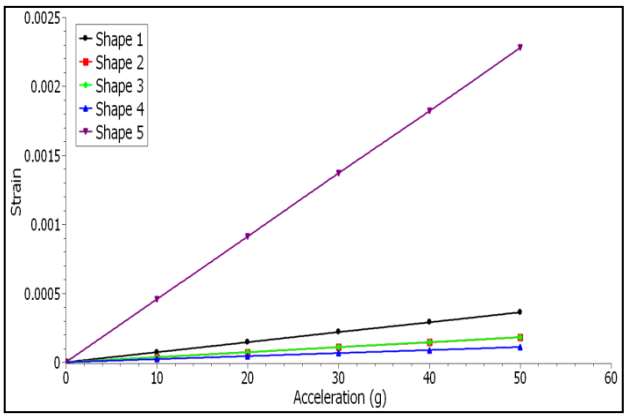

Figure 5: The comparison of strain for all five shapes for 0-50 g acceleration

B. Modal Analysis Simulation Results

Natural frequency is determined by performing modal analysis for each shape of accelerometer structures. Figure 6 shows the natural frequency and mechanical sensitivity of five shapes structures under 0-50 g acceleration. As depicted in Figure 6, structure number 4 shows the highest natural frequency value, of 6.79 kHz followed by shape number 2, 3, 1 and 5 with natural frequency values of 2.04 kHz, 2.01 kHz, 1.44 kHz and 0.17 kHz respectively. Meanwhile, for mechanical sensitivity, the highest sensitivity starts from shape number 5 with value of 9.21 x 10^{-7} $(rad/s)^{-2}$ followed by 1, 3, 2 and 4 with mechanical sensitivity values of 1.23 x 10^{-8} $(rad/s)^{-2}$, 6.24 x 10^{-9} $(rad/s)^{-2}$, 6.10 x 10^{-9} $(rad/s)^{-2}$ and 5.50 x 10^{-10} $(rad/s)^{-2}$ respectively. It can be observed that the sensitivity of accelerometer structures is inversely proportional to the angular natural frequency as shown by Equation (4).

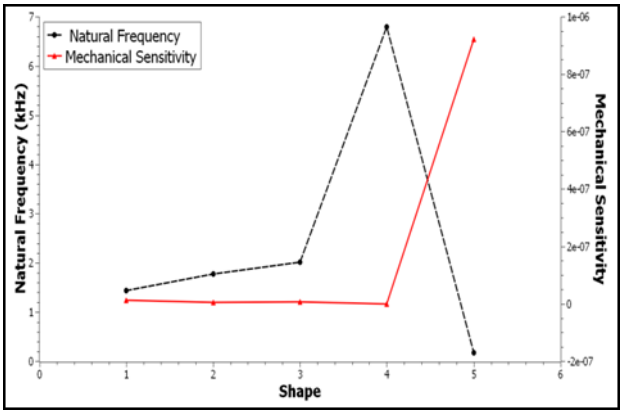

Figure 6: The comparison of natural frequency and mechanical sensitivity for all five shapes for 0-50 g acceleration

C. Comparative Analysis of Shape 1 To 5

In order to design high performance accelerometer sensors, the structures with maximum stress is preferred because it will give higher sensitivity. This is due to the piezoresistor resistance changes that are proportional to the applied stress. Therefore if the piezoresistor is placed where the maximal stress is located on the beams, the highest sensitivity is then obtained. However, the sensor sensitivity and bandwidth are inversely proportional. Thus, resonant frequency has to be lowered to achieve higher prime-axis sensitivity, but at the same time it should be kept well above the operating frequency range of the device [21]. Typically, the usable bandwith is five times smaller than the natural frequency [19]. So, the minimum natural frequency of 2 kHz is chosen as a hard constraint in order to obtain a bandwidth at least of 400 Hz (see specifications in Table 1). From Table 3, it can be seen that the value of the natural frequency of shape 5 is the lowest value amongst five shapes with only 170 Hz even it gives the highest stress at its beams. This is below the operating frequency range for this application. It may be noted from the simulation results that the natural frequency of Shape 1 which is 1.44 kHz is also below the minimum natural frequency requirements. Shape 4 predominates the natural frequency to 6.79 kHz; by contrast to the other hand, it has the lowest sensitivity compared to the other shapes. Meanwhile, the shape number 2 and 3 has demonstrated more than acceptable natural frequency with 2.04 kHz and 2.01 kHz respectively. In addition, the maximum stress for both structures looks promising for airbag applications.

Table 3
Performance Comparison of Stress, Displacement, Strain, Natural Frequency and Mechanical Sensitivity of shape 1 to 5

Shape	Accel.Axis (Load: ±50 g)	Maximum Stress (N/m^2)	Total Displacement (μm)	Strain	Natural Frequency (kHz)	Mechanical Sensitivity $(rad/s)^{-2}$
1	x	2.89×10^7	2.03	9.06×10^{-5}	1.44	1.23×10^{-8}
	y	4.28×10^7	4.10	1.59×10^{-4}		
	z	7.11×10^7	6.02	3.62×10^{-4}		
2	x	1.33×10^7	0.94	6.47×10^{-5}	2.04	6.10×10^{-9}
	y	1.97×10^7	1.39	9.26×10^{-5}		
	z	3.48×10^7	2.99	1.81×10^{-4}		
3	x	1.84×10^7	1.38	9.42×10^{-5}	2.01	6.24×10^{-9}
	y	1.92×10^7	1.38	8.85×10^{-5}		
	z	3.52×10^7	3.07	1.81×10^{-4}		
4	x	1.54×10^7	0.19	1.81×10^{-4}	6.79	5.50×10^{-10}
	y	1.54×10^7	0.19	1.81×10^{-4}		
	z	2.30×10^7	0.30	1.81×10^{-4}		
5	x	2.55×10^8	175	9.38×10^{-4}	0.17	9.21×10^{-7}
	y	2.52×10^8	176	7.98×10^{-4}		
	z	6.78×10^8	458	2.28×10^{-3}		

IV. Conclusion and Future Work

The design and analysis of MEMS piezoresistive accelerometer structure for airbag application has been presented in this paper. Five different shapes were studied with common proof mass volume. From the study, the stucture with the proof mass is suspended by eight beams has been identified fulfill the minimum requirements for natural frequency in order to achieve bandwidth range 0 - 400 Hz with high sensitivity at approximately 6×10^{-9} $(rad/s)^{-2}$. The strategic locations in placing the piezoresistors for greater sensitivity has been recognized. These results would be useful to find the most effective and optimum design of a MEMS high sensitive accelerometer sensor. However, this analysis is still at an early stage, there are more important factors could affect the performance of the sensor such as the size of the structures, including proof mass and beams; and the placement or location of the beams. The piezoresistors' design and material will also give a big effect on the sensors performance. Hence, these parameters should be comprehensively studied in order to design a highly sensitive MEMS Piezoresistive that satisfies the requirements of an accelerometer meant for airbag sensor applications.

Acknowledgment

The authors would like to thank the Ministry of Higher Education (MOHE), Malaysia for the financial support under RAGS grant (RAGS/2013/UNISZA/SG02/1) and Advanced Technology Cluster, UniSZA for its support.

References

[1] N. Yazdi, F. Ayazi, and K. Najafi. "Micromachined inertial sensors," *Proceedings of the IEEE*, vol. 86, no. 8, pp. 1640–1659, 1998.

[2] A.Ravi Sankar, S.Das, S.K Lahiri. "Cross-axis sensitivity reduction of a silicon MEMS piezoresistive accelerometer," *Microsystem Technologies*, vol. 15, pp. 511–518, 2009.

[3] M. Messina, J. Njuguna, V. Dariol, C. Pace, and G. Angeletti, "Design and simulation of a novel biomechanic piezoresistive sensor with silicon nanowires," *IEEE/ASME Trans. Mechatronics*, vol. 18, no. 3, pp. 1201–1210, 2013.

[4] G. Ionascu, A. Sandu, L. Bogatu, C. D. Comeaga, E. Manea, and D. Besnea, "Simulation Aspects of Performance and Experimental Procedures for a microaccelerometer," *U.P.B.Sci.Bull.,Series D*, vol. 74, 2012.

[5] M. C. Mathew, J. G. Jency, and P. G. Scholar, "A Review on Optimized Accelerometer Design for High Performance Application," *International Journal of Computer Applications*, no. 0975–8887, pp. 32–37, 2013.

[6] T. D.Tran. "Optimum Design Considerations for a 3-DOF Micro Accelerometer Using Nanoscale Piezoresistors," *3rd IEEE Int. Conf. on Nano/Micro Engineered and Molecular Systems*, pp. 770–773, 2008.

[7] D. V. Dao, S. Okada, V. T. Dau, T. Toriyama, and S. Sugiyama, "Development of a 3-DOF silicon piezoresistive micro accelerometer," *Proceedings of the 2004 Int. Symp. on Micro-Nanomechatronics and Human Science and The Fourth Symp. Micro-Nanomechatronics for Information-Based Society*, pp. 1–6, 2004.

[8] S.Kavitha, R. J. Daniel, and K. Sumangala, "Computer Aided Design and Effects of Beam Placement in Bulk Micromachined Piezoresistive MEMS Accelerometer for Concrete SHM Applications," *Procedia Engineering*, vol. 38, pp. 2033–2047, 2012.

[9] Yi Luo. "Cross Axis Sensitivity Enhancement For A Quad Beam Piezoresistive Accelerometer," *26th IEEE Canadian Conference Of Electrical And Computer Engineering (CCECE)*,vol. 6, pp. 5–8, 2013.

[10] A. Benichou, "Study of a Three-Axis Piezoresistive Accelerometer," *Proceedings of the 1st Annual International Interdisciplinary Conference, AIIC*, no. 1, pp. 24–26, 2013.

[11] C. Du, C. He, J. Yu, X. Ge, Y. Zhang, and W. Zhang, "Design and measurement of a piezoresistive triaxial accelerometer based on MEMS technology," *Journal of Semiconductors*., vol. 33, no. 10, p. 104005, 2012.

[12] K.H. Kim, J.S. Ko, C. Young-Ho, K. Lee, B.M. Kwak, K. Park, "A skew-symmetric cantilever accelerometer for automotive airbag applications," *Sensors and Actuators A*, no. 50., pp.121-126, 1995.

[13] Y. C. Tang, Bin, Shiwei Xi, Mingqiu Yao, De Zhang, Kazuo Sato, Guofen Xie, Wei Su. "Fabrication of A Symmetrical Accelerometer Structure," *Proceedings of the IEEE* , pp 1-6 , April 2014.

[14] M. Messina and J. Njuguna, "Potential of silicon nanowires structures as nanoscale piezoresistors in mechanical sensors," *IOP Conf. Ser. Mater. Sci. Eng.*, vol. 40, p. 012038, 2012.

[15] H. Chen, M. Bao, H. Zhu, and S. Shen, "A piezoresistive accelerometer with a novel vertical beam structure," *Sensors Actuators A Phys*., vol. 63, no. 1, pp. 19–25, 1997.

[16] M. H. M. Khir, P. Qu, and H. Qu, "A low-cost CMOS-MEMS piezoresistive accelerometer with large proof mass," *Sensors (Basel).*, vol. 11, no. 8, pp. 7892–907, 2011.

[17] W. Benecke, "Micromechanical sensors," *Proceedings. VLSI Computer. Peripherals, COMPEURO 89*, pp. 1–20, 1989.

[18] K. Naeli, Optimization of Piezoresistive Cantilevers for Static and Dynamic Sensing Applications, 2009.

[19] M. Messina, "Design and optimization of a novel tri-axial miniature ear plug piezoresistor accelerometer with nanoscale piezoresistors,".

[20] J. Wang, X. Xia, and X. Li. "Monolithic Integration of Pressure Plus Acceleration Composite TPMS Sensors With a Single-Sided Micromachining Technology," *Journal of Microelectromechanical Systems*., vol. 21, no. 2, pp. 284–293, 2012.

[21] A. R. Sankar, J. G. Jency, and S. Das, "Design, fabrication and testing of a high performance silicon piezoresistive Z-axis accelerometer with proof mass-edge-aligned-flexures," *Microsystem technologies*., vol. 18, no. 1, pp. 9–23, 2011.